Supplementary Material

Composition-regulated lattice strain of PdSn/C for boosting C1 pathway in ethanol electrooxidation

**Yin Cai[1,#], Yi Tao[1,#], Jie Ding[2], Fuhua Li[3], Rongsheng Chen[1], Tao Ma[1,*], Feng Liang[1,*]**

[1]The State Key Laboratory of Refractories and Metallurgy, School of Chemistry and Chemical Engineering, Wuhan University of Science and Technology, Wuhan 430081, Hubei, China.

[2]Department of Materials Science and Engineering, City University of Hong Kong, Hong Kong, SAR 999077, China.

[3]School of Chemistry and Chemical Engineering, Chongqing Key Laboratory of Theoretical and Computational Chemistry, Chongqing University, Chongqing 401331, China.

[#]Authors contributed equally.

Correspondence to: Dr. Tao Ma, The State Key Laboratory of Refractories and Metallurgy, School of Chemistry and Chemical Engineering, Wuhan University of Science and Technology, No. 947, Heping Avenue, Qingshan District, Wuhan 430081, Hubei, China. E-mail: taoma01@wust.edu.cn; Prof. Feng Liang, The State Key Laboratory of Refractories and Metallurgy, School of Chemistry and Chemical Engineering, Wuhan University of Science and Technology, No. 947, Heping Avenue, Qingshan District, Wuhan 430081, Hubei, China. E-mail: feng_liang@whu.edu.cn
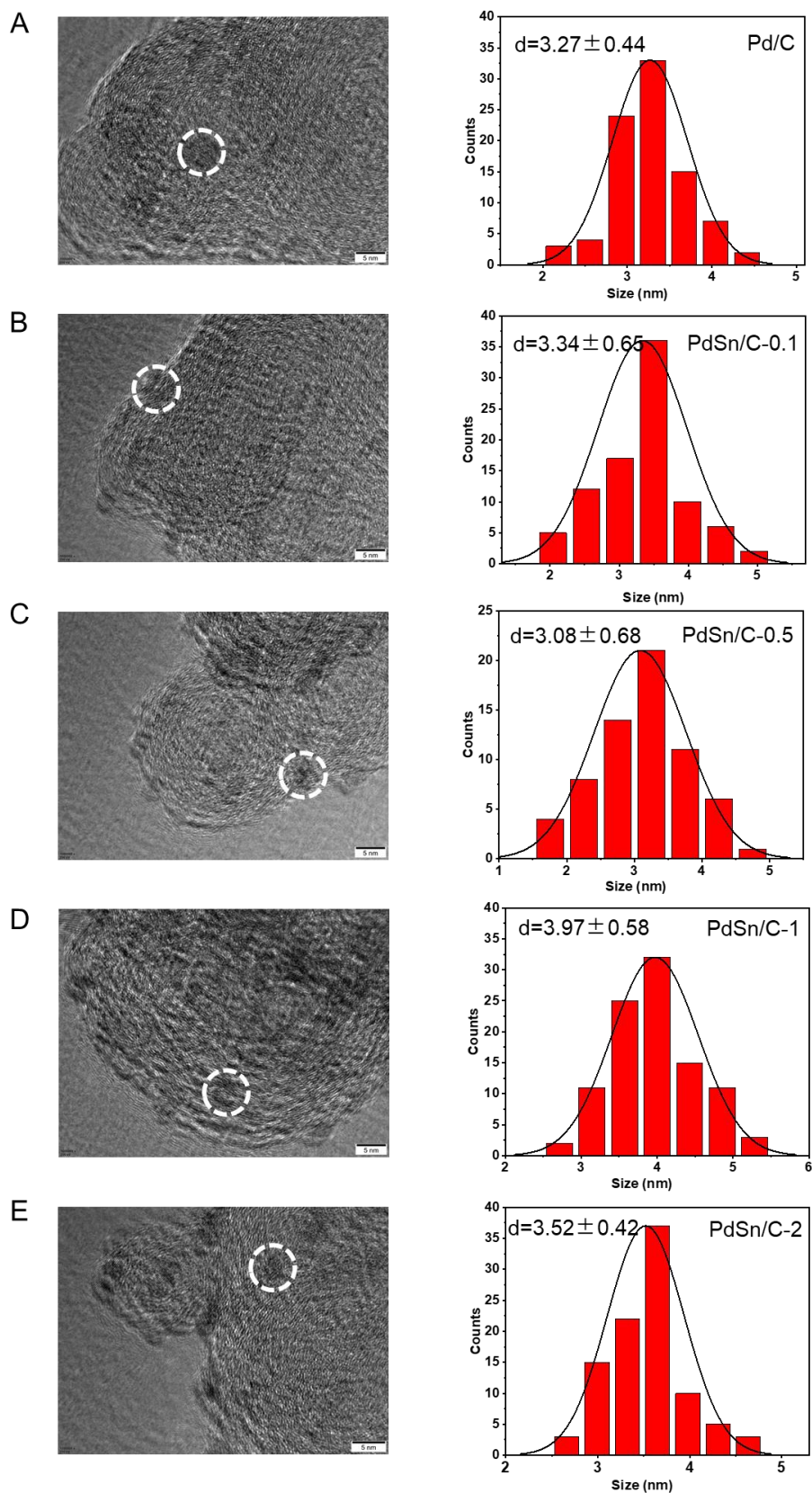
Figure S1. High-magnification TEM images (left) and size distribution (right) of (A) Pd/C, (B) PdSn/C-0.1, (C) PdSn/C-0.5, (D) PdSn/C-1, (E) PdSn/C-2. The scale in TEM image is 5 nm.
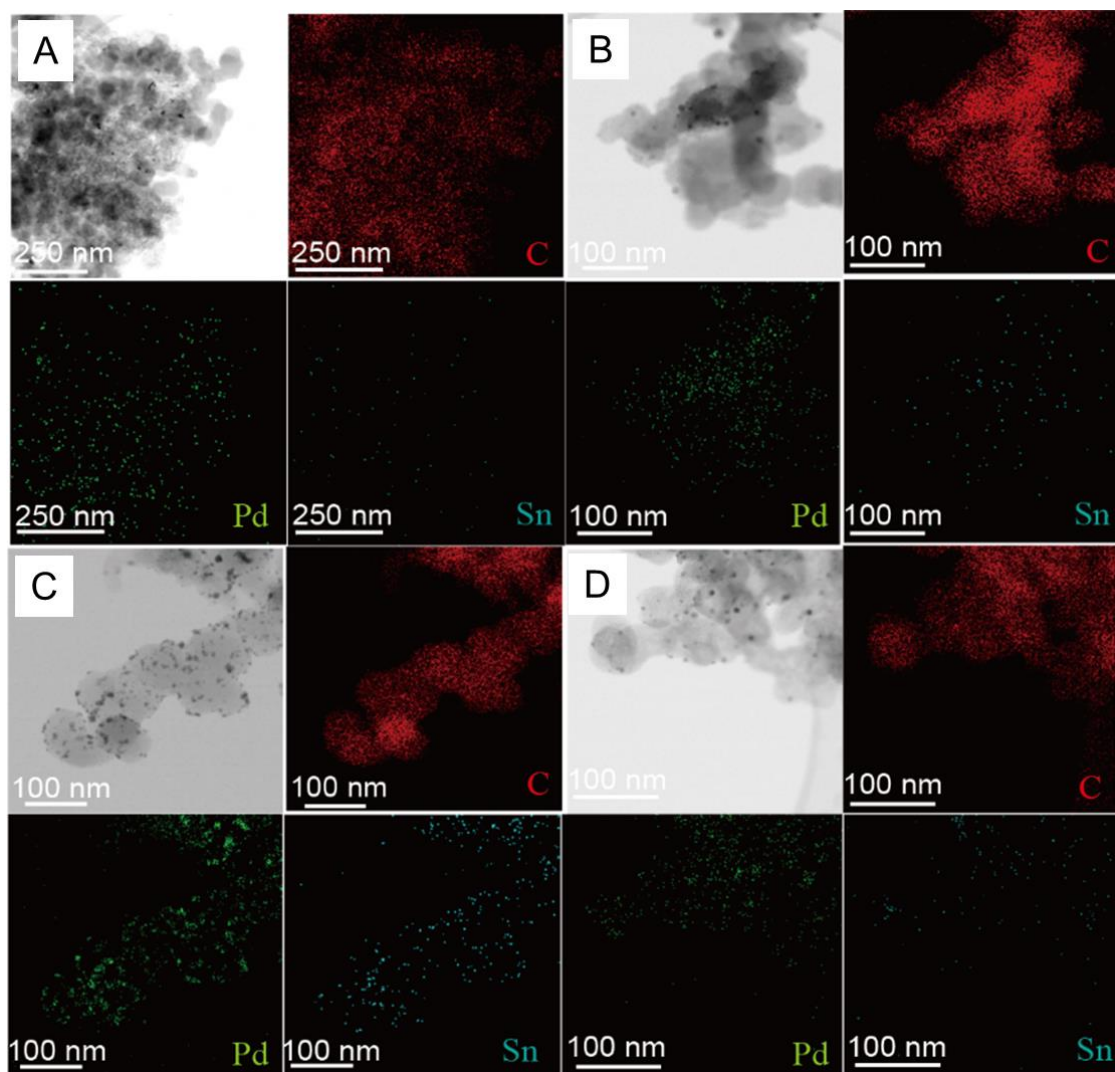
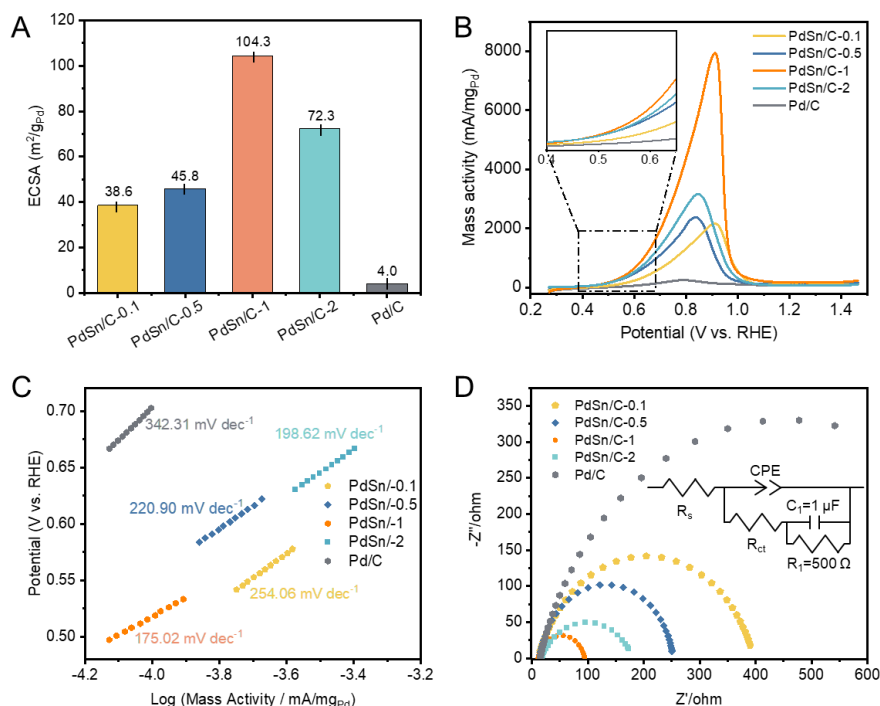**Figure S2.** TEM images and corresponding EDS mappings of (A) PdSn/C-0.1, (B) PdSn/C-0.5, (C) PdSn/C -1, and (D) PdSn/C-2.
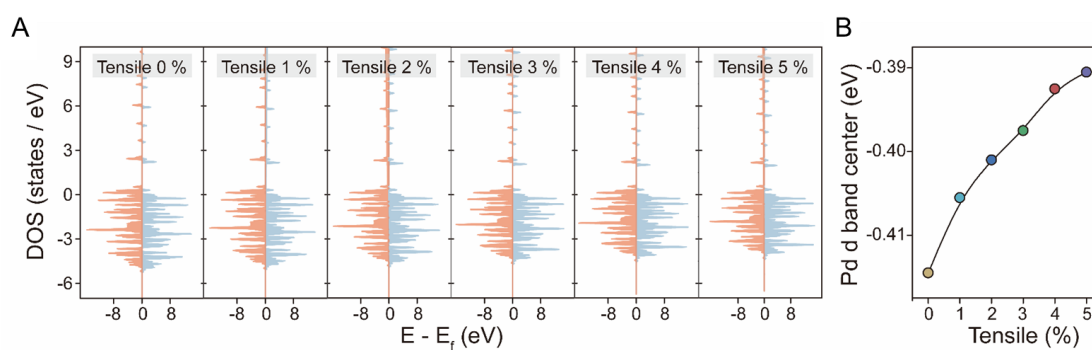

Figure S3. (A) The density of states (DOS) for Pd alloy with different tensile effect, (B) the change of d-band center due to strain of the Pd (111) facet.
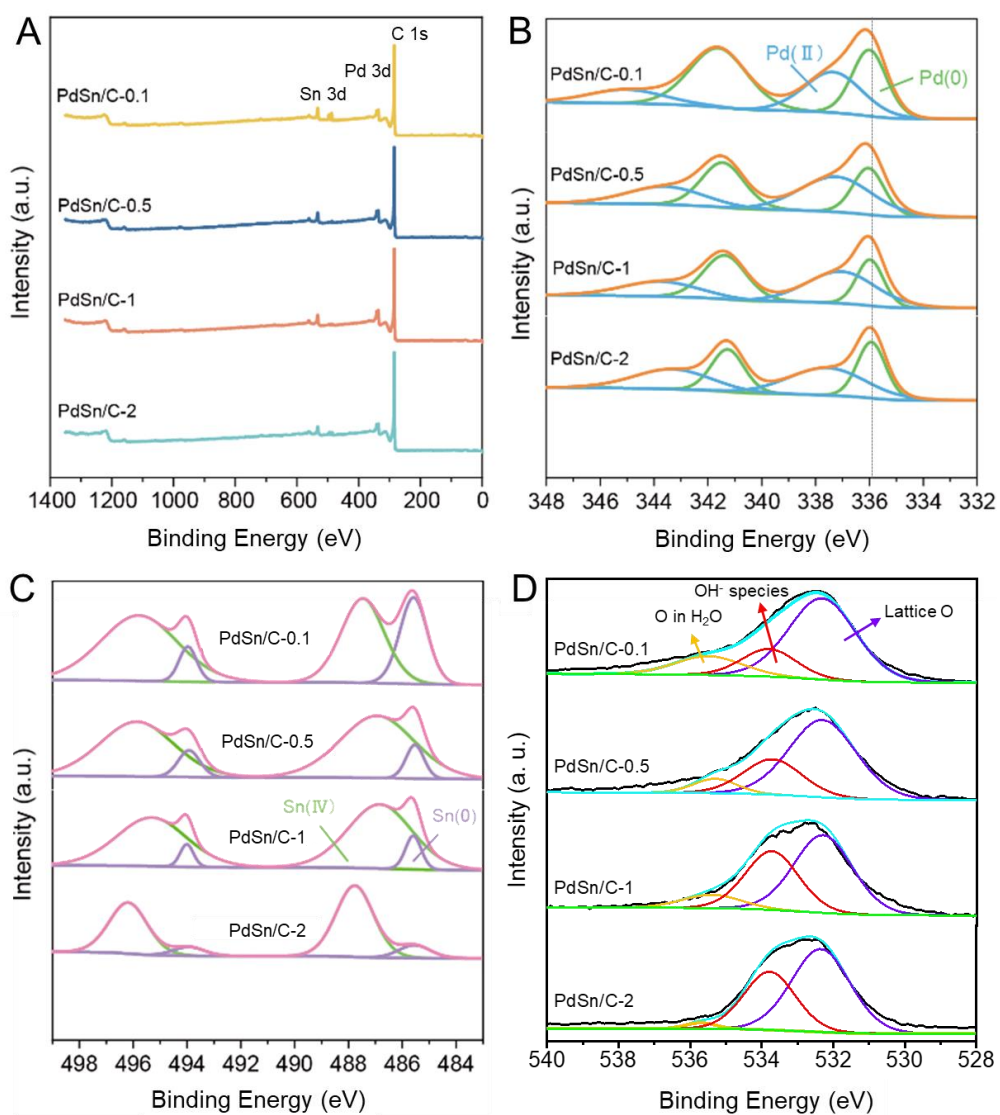
Figure S4. (A) Wide scan XPS spectra of PdSn/C-X, and its high-resolution region of (B) Pd 3d, (C) Sn 3d, and (D) O 1s.

Figure S5. (A) Summarized ECSAs of different PdSn/C-X and Pd/C in 1.0 M KOH, (B) LSV curves, (C) Tafel plots, and (D) Nyquist plots of different PdSn/C-X and Pd/C collected in 1.0 M KOH and 1.0 M ethanol. The insets in (B) and (D) are the magnified view around onset potential and the equivalent circuit model used to fit the Nyquist plots, respectively.
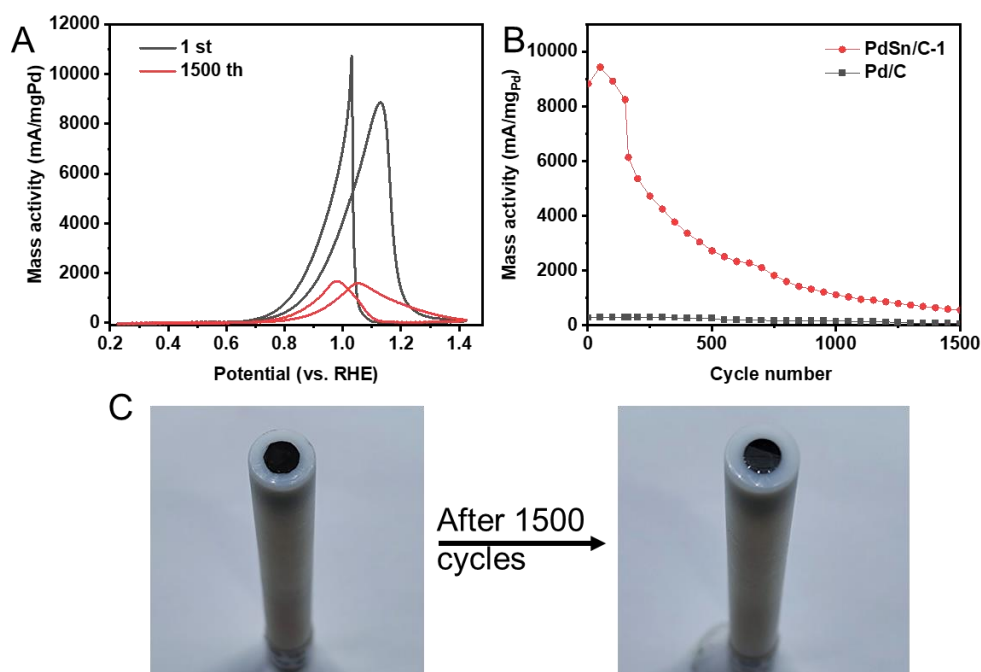
Figure S6. (A) The CVs before and after 1500 sweeps of PdSn/C-1 recorded in 1.0 M KOH with 1.0 M ethanol solution at scan rate of 50 mV/s. (B) The plots of forward peak current density of PdSn/C-1 and Pd/C based on 1500 sweeps. (C) The PdSn/C-1 loaded GCE before and after 1500 sweeps.
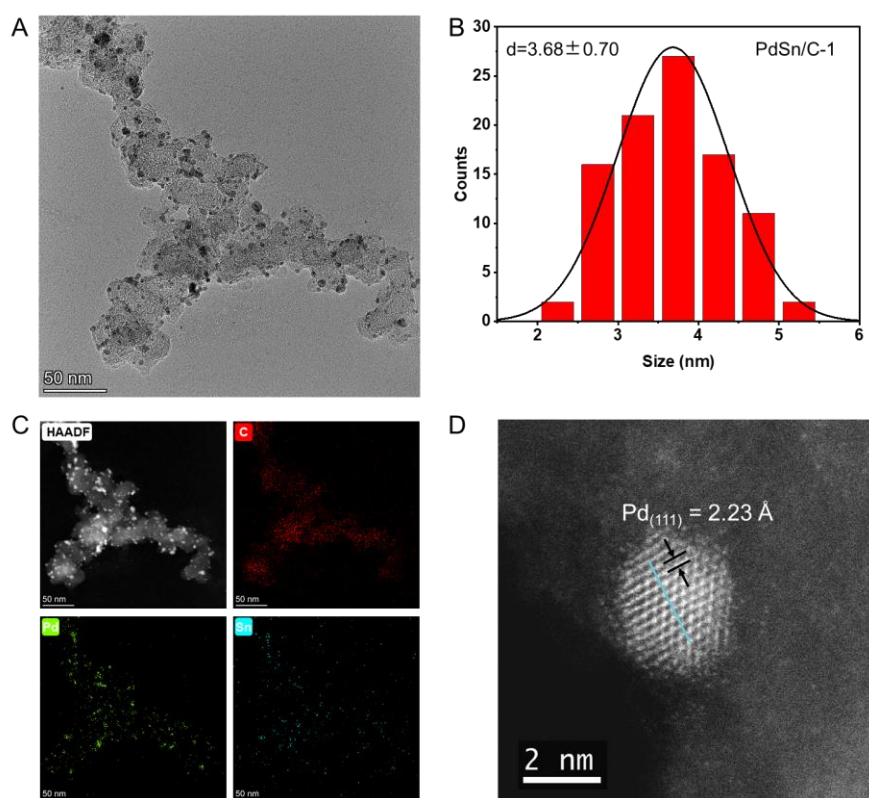
Figure S7. (A) TEM image, (B) size distribution, (C) corresponding EDS mappings, and (D) HAADF-STEM image of PdSn/C-1 after 1500 sweeps.
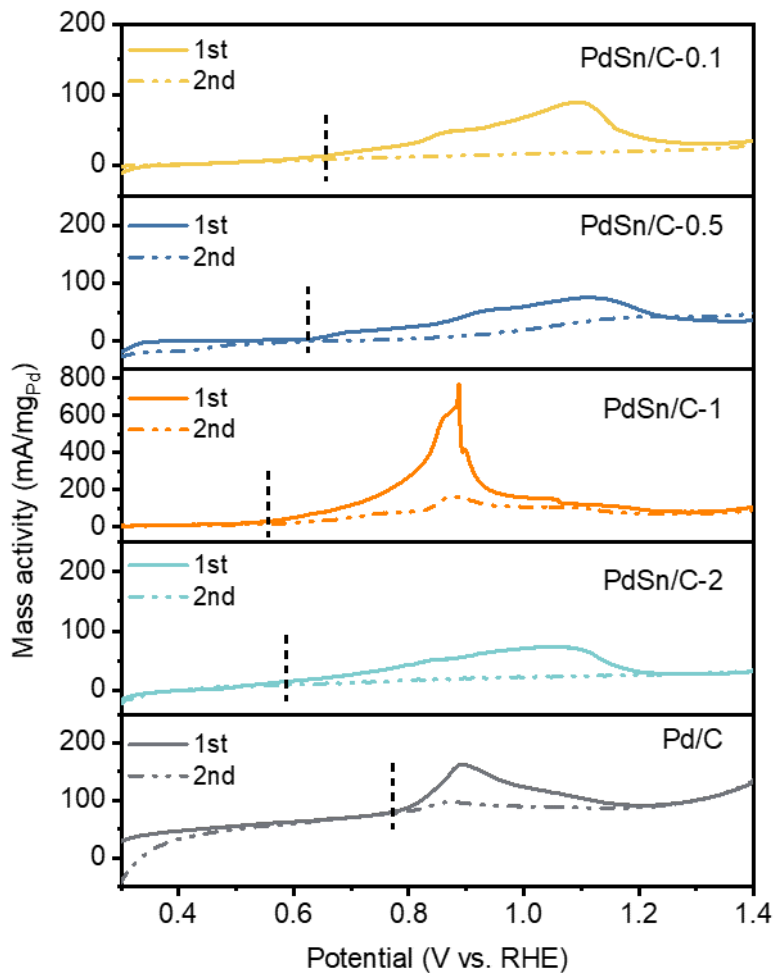
Figure S8. CO stripping voltammograms of PdSn/C-X and Pd/C obtained in 1.0 KOH.
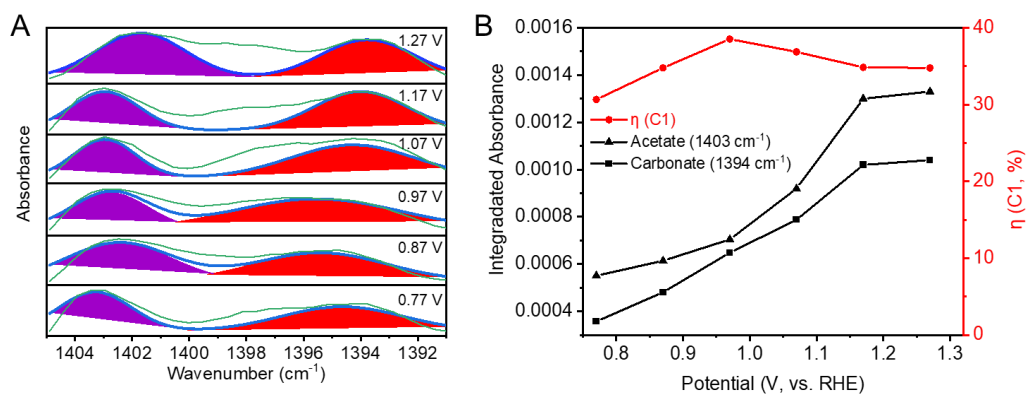
Figure S9. (A) The fitted bands (corresponding to Figure 4B) at 1405 to 1391 cm^{-1} of PdSn/C-1, (B) the corresponding integrated absorbances of the peaks around 1394 and 1403 cm^{-1} (left axis) and selectivity to C1 (right axis) for PdSn/C-1.
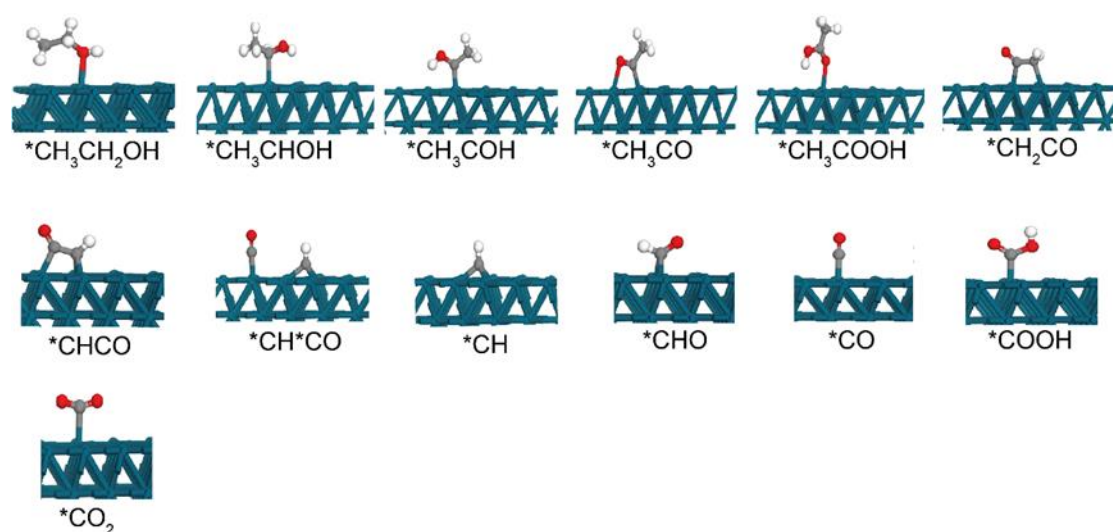
Figure S10. The atomic structures of reaction intermediates during EOR on the Pd (111) surface.

Table S1. Element content of as-prepared catalysts according to ICP-MS analysis

Catalysts	Pd (mg/L)	Sn (mg/L)	C (mg/L)	Pd (%)	Sn (%)	Sn/Pd (mol)
PdSn/C-0.1	431.53	34.50	2491.68	14.59	1.17	1:14
PdSn/C -0.5	510.44	46.32	3112.83	13.91	1.26	1:12
PdSn/C -1	399.09	94.951	3995.16	8.89	2.12	1:5
PdSn/C -2	428.56	109.94	2520.46	14.01	3.59	1:4
Pd/C	456.82	0	2227.28	17.02	0	0:1

Table S2. Comparison of the electrochemical performance of various nanomaterials for EOR in alkaline media

Catalyst	Method	Electrolyte	Mass activity (mA/mg$_{Pd}$)	ECSA (m^2/g$_{Pd}$)	Stability	Ref.
PdAg	Hydrothermal	1.0 M KOH and 1.0 M ethanol	1950	24.2	342 mA mg^{-1} after 1000 s.	[4]
Pd/NiMoO$_4$	Hydrothermal	1.0 M KOH and 1.0 M ethanol	3250	174.2	10.62 mA cm^{-2} after 10,000 s	[5]
PdSn:P/C	One-pot	0.5 M KOH and 0.5 M ethanol	5030	120.1	9.52 mA cm^{-2} after 7000s	[6]
PdAg@Pd	One-pot	1.0 M KOH and 1.0 M ethanol	3480	28.11	190.6 mA mg$_{Pd}$ after 3600s	[7]
PdAuPt	Surfactant-free method	1.0 M KOH and 1.0 M	4990	62.92	92% After 500 cycles	[8]

		ethanol				
PdBP	One-step aqueous	1.0 M KOH and 1.0 M ethanol	4150	35	1870 mA mg$_{Pd}$ after 5000 cycles	[9]
PdPb	One-step hydrothermal	1.0 M KOH and 1.0 M ethanol	3460	62	1497 mA mg$_{Pd}$ after 1000s	[10]
PdPtBi	Hydrothermal	1.0 M KOH and 1.0 M ethanol	11080	12	47.2% after 3,600 s	[11]
PtAg	Hydrothermal	1.0 M KOH and 1.0 M ethanol	6100	21.8	152 mA mg$_{Pd}$ after 6000s	[12]
AgPdPt	One-pot	1.0 M KOH and 1.0 M ethanol	7240	103.8	289mA mg$_{Pd}$ after for 7200 s	[13]
PdSn/TiO$_2$	Co-reduction	1.0 M NaOH and 1.0M ethanol	3381	NA	decay only 20% after 300 cycles	[14]
PdZn	Hydrothermal	1.0 M KOH and 1.0M ethanol	18140	77.51	no change in the CV curves after 2000 cycles	[15]
PdSn/rgo	Seed-mediated	1.0 M KOH and 1.0M ethanol	2701	23.6	1187 mA mg^{-1} retained after 500 cycles	[16]
PdNN	Hydrothermal	1.0 M KOH and 1.0M ethanol	2040	100	87.6% after the 1000th cycle	[17]
PdSn/C-1	Co-reduction at room temperature	1.0 M KOH and 1.0 M ethanol	8452	104.3	1600 mA mg^{-1} after 1500 s	This work

Table S3. The fitted parameters in equivalent circuit model of catalysts

Nanoparticles	R_{ct} (Ω)	R_s (Ω)
PdSn NPs-0.1	385	12.3
PdSn NPs-0.5	139	14.1
PdSn NPs-1	83	11.5
PdSn NPs-2	165	17.0
Pd/C	882	14.4

References

[1] M.C. Hidalgo, J.J. Murcia, J.A. Navío, G. Colón, Photodeposition of Gold on Titanium Dioxide for Photocatalytic Phenol Oxidation, Appl. Catal., A, 397 (2011) 112.

[2] M. Maicu, M.C. Hidalgo, G. Colon, J.A. Navio, Comparative Study of the Photodeposition of Pt, Au and Pd on Pre-sulphated TiO2 for the Photocatalytic Decomposition of Phenol, J. Photochem. Photobiol., A, 217 (2011) 275.

[3] A. Primo, A. Corma, H. Garcia, Titania Supported Gold Nanoparticles as Photocatalyst, Phys. Chem. Chem. Phys., 13 (2011) 886.

[4] L. Yang, F. Gao, L. Xu, B. Fu, Y. Zheng, P. Guo, Bimetallic Face-Centered Cubic Pd–Ag Nano-dendritic Alloys Catalysts Boost Ethanol Electrooxidation, ACS Applied Energy Materials, 5 (2022) 11624-11631.

[5] M. Wang, D. Li, Y. Tian, J. Zhao, Z. Yue, X. Wang, X. Ma, J. Wang, T. Hu, J. Jia, H.-S. Wu, Pd Nanoparticles Coupled to NiMoO4–C Nanorods for Enhanced Electrocatalytic Ethanol Oxidation, ACS Applied Materials & Interfaces, 13 (2021) 53777-53786.

[6] X. Yu, J. Liu, J. Li, Z. Luo, Y. Zuo, C. Xing, J. Llorca, D. Nasiou, J. Arbiol, K. Pan, T. Kleinhanns, Y. Xie, A. Cabot, Phosphorous incorporation in Pd2Sn alloys for electrocatalytic ethanol oxidation, Nano Energy, 77 (2020) 105116.

[7] H. You, F. Gao, T. Song, Y. Zhang, H. Wang, X. Liu, M. Yuan, Y. Wang, Y. Du, Tunable long-chains of core@shell PdAg@Pd as high-performance catalysts for ethanol oxidation, Journal of Colloid and Interface Science, 574 (2020) 182-189.

[8] K. Guo, Y. Teng, R. Guo, Y. Meng, D. Fan, Q. Hao, Y. Zhang, Y. Li, D. Xu, Engineering ultrathin PdAu nanoring via a facile process for electrocatalytic ethanol oxidation, Journal of Colloid and Interface Science, 628 (2022) 53-63.

[9] H. Lv, L. Sun, D. Xu, B. Liu, Ternary metal-metalloid-nonmetal alloy nanowires: a novel electrocatalyst for highly efficient ethanol oxidation electrocatalysis, Science Bulletin, 65 (2020) 1823-1831.

[10] N. Ma, S. Wang, X. Liu, Y. Sun, Y. Yin, L.Y. Zhang, P. Guo, PdPb bimetallic nanowires as electrocatalysts for enhanced ethanol electrooxidation, Science China Materials, 63 (2020) 2040-2049.

[11] N. Qian, L. Ji, J. Li, H. Zhang, D. Yang, PdPtBi networked nanowires derived from Pd nanosheets as efficient catalysts for ethanol oxidation, Nano Research, 16 (2023) 9125-9131.

[12] X. Fu, C. Wan, A. Zhang, Z. Zhao, H. Huyan, X. Pan, S. Du, X. Duan, Y. Huang, Pt3Ag alloy wavy nanowires as highly effective electrocatalysts for ethanol oxidation reaction, Nano Research, 13 (2020) 1472-1478.

[13] H. Wang, S. Jiao, S. Liu, K. Deng, H. Yu, X. Wang, Y. Xu, Z. Wang, L. Wang, Ultrafine PdAgAu alloy nanowires for ethanol oxidation electrocatalysis, Journal of Materials Chemistry A, 10 (2022) 24051-24055.

[14] X. Wang, W. Fan, C. Zhang, M. Chi, A. Zhu, Q. Zhang, Q. Liu, Well-dispersed Pd–Sn nanocatalyst anchored on TiO2 nanosheets with enhanced activity and durability for ethanol electarooxidation, Electrochimica Acta, 320 (2019) 134588.

[15] Y. Qiu, J. Zhang, J. Jin, J. Sun, H. Tang, Q. Chen, Z. Zhang, W. Sun, G. Meng, Q.

Xu, Y. Zhu, A. Han, L. Gu, D. Wang, Y. Li, Construction of Pd-Zn dual sites to enhance the performance for ethanol electro-oxidation reaction, Nature Communications, 12 (2021) 5273.

[16] J. Huang, L. Ji, X. Li, X. Wu, N. Qian, J. Li, Y. Yan, D. Yang, H. Zhang, Facile synthesis of PdSn alloy octopods through StranskiKrastanov growth mechanism as electrocatalysts towards ethanol oxidation reaction, CrystEngComm, 24 (2022) 3230-3238.

[17] H. Begum, M.S. Ahmed, S. Jeon, Highly Efficient Dual Active Palladium Nanonetwork Electrocatalyst for Ethanol Oxidation and Hydrogen Evolution, ACS Applied Materials & Interfaces, 9 (2017) 39303-39311.